Supplementary Information

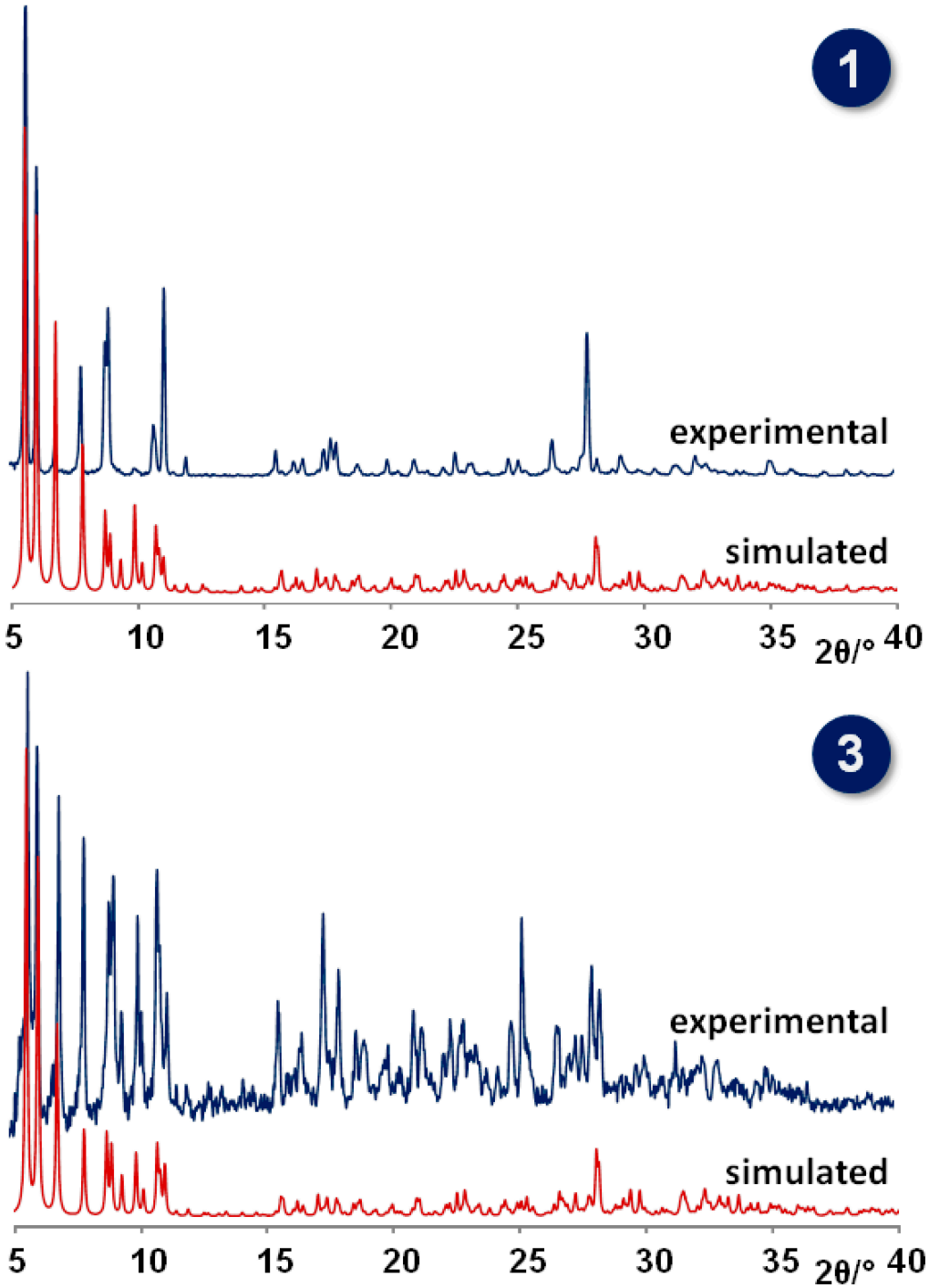

Figure S1. Experimental powder X-ray diffraction patterns of compounds **1** and **3** compared to those simulated from single-crystal X-ray diffraction data.

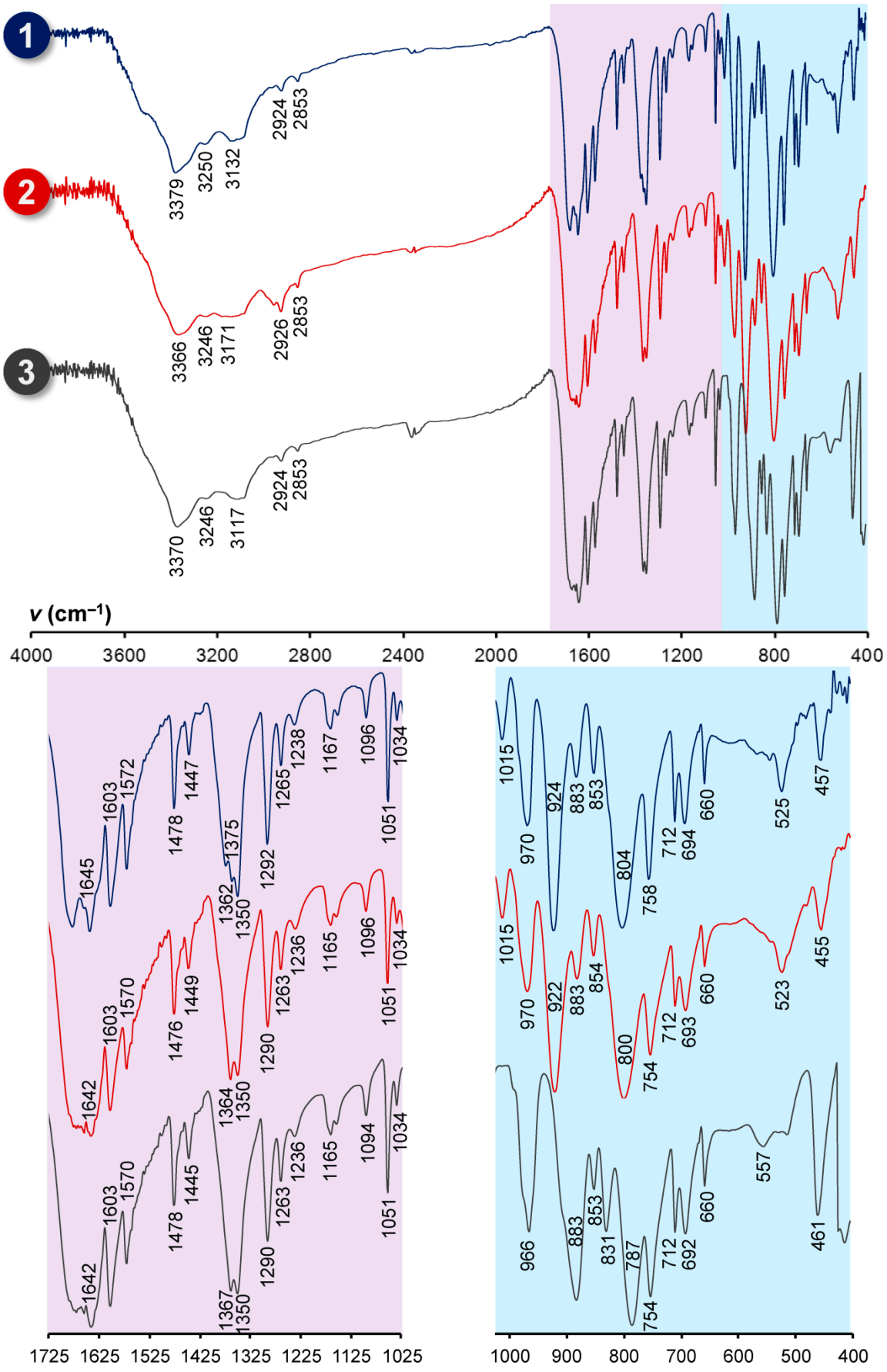

Figure S2. Infrared spectra of compounds **1**–**3** with details of the metalorganic and inorganic regions (framed in violet and blue, respectively).

Table S1. Ranges of bond lengths, (mean) values and selected interatomic distances (Å) in the Keggin clusters of **1**–**3** and their anhydrous derivatives **1a** and **3a** compared to those of the DFT-optimized species (opt) [a].

$[SiW_{12}O_{40}]^{4-}$	**1**	**1a**	**2**	**opt**
W–O$_c$	2.316(12)–2.462(12) (2.383)	2.350(12)–2.478(12) (2.398)	2.26(3)–2.53(4) (2.38)	2.325
W–O$_b$	1.690(15)–2.108(13) (1.926)	1.741(12)–2.067(13) (1.920)	1.59(4)–2.20(5) (1.92)	1.916, 1.937
W–O$_t$	1.629(14)–1.773(16) (1.702)	1.631(16)–1.748(15) (1.693)	1.58(5)–1.81(6) (1.70)	1.743
X–O$_c$	1.569(12)–1.683(12) (1.625)	1.591(11)–1.686(12) (1.629)	1.54(4)–1.74(4) (1.64)	1.667
X⋯W	3.516(1)–3.541(1) (3.529)	3.525(1)–3.538(1) (3.532)	3.498(6)–3.545(6) (3.526)	3.588
W⋯W$_{trans}$	7.032(1)–7.082(1) (7.058)	7.045(1)–7.077(1) (7.064)	7.042(1)–7.061(2) (7.052)	7.172
$[GeW_{12}O_{40}]^{4-}$	**3**	**3a**		**opt**
W–O$_c$	2.290(12)–2.425(13) (2.354)	2.28(2)–2.44(2) (2.34)		2.345
W–O$_b$	1.733(13)–2.123(13) (1.939)	1.72(2)–2.13(3) (1.92)		1.928, 1.940
W–O$_t$	1.653(15)–1.727(17) (1.691)	1.51(3)–1.83(3) (1.70)		1.740
X–O$_c$	1.679(12)–1.777(12) (1.728)	1.70(2)–1.83(2) (1.75)		1.738
X⋯W	3.527(1)–3.548(1) (3.539)	3.530(1)–3.549(1) (3.538)		3.592
W⋯W$_{trans}$	7.053(1)–7.096(1) (7.077)	7.060(1)–7.097(1) (7.076)		7.180

[a] San Felices, L.; Vitoria, P.; Gutiérrez-Zorrilla, J.M.; Lezama, L.; Reinoso, S. *Inorg. Chem.* **2006**, *45*, 7748–7757.

Table S2. Donor···acceptor distances (Å) for the N–H···O and O–H···O hydrogen bonds in **1** and **3** and their anhydrous derivatives **1a** and **3a**.

Donor···Acceptor	1	1a	3	3a
N1G···O1C^{i}	3.059(14)	3.213(13)	3.066(13)	3.20(3)
N1G···O2C^{i}	3.366(16)	3.479(14)	3.362(15)	3.49(3)
N1G···O4/O4Z^{ii}	–	2.941(19)/2.90(2)	–	2.85(4)/2.91(4)
N1G···O4w^{i}	2.875(15)	–	2.882(15)	–
N2G···O2C	2.822(14)	2.832(14)	2.814(14)	2.83(3)
N2G···O1A	3.322(12)	3.195(12)	3.335(12)	3.17(2)
N2G···O2A	3.042(12)	3.057(13)	3.058(13)	3.10(3)
N3G···O2A	3.059(13)	2.916(13)	3.075(14)	2.96(3)
N3G···O2B^{iii}	3.070(14)	2.871(12)	3.084(13)	2.85(3)
N3G···O3w^{ii}	3.29(3)	–	3.26(3)	–
N4G···O3A	3.068(11)	3.134(12)	3.077(12)	3.10(2)
N4G···O4A	3.444(13)	3.495(13)	3.435(13)	3.48(2)
N4G···O4C^{iii}	2.865(13)	2.863(13)	2.876(12)	2.89(3)
N5G···O3B^{iv}	2.963(12)	2.885(12)	2.968(12)	2.93(2)
N5G···O4A	2.847(12)	2.800(12)	2.842(13)	2.82(2)
N6G···O4B^{iv}	2.856(13)	2.852(11)	2.861(12)	2.88(2)
N6G···O3C^{iii}	2.956(12)	2.982(12)	2.960(12)	2.94(2)
N6G···O4C^{iii}	3.435(13)	3.351(13)	3.435(13)	3.31(3)
O1w···O1w^{v}	2.763(13)	–	2.761(12)	–
O1w···O2w^{v}	2.724(17)	–	2.727(15)	–
O1w···O3w	2.94(2)	–	2.95(2)	–
O2w···O5w	2.98(5)	–	3.14(4)	–
O2w···O6	2.87(2)	–	2.91(2)	–
O2w···O2A^{vi}	2.746(17)	–	2.731(17)	–
O4w···O2B^{vii}	2.720(13)	–	2.723(13)	–
O4w···O4Z^{viii}	2.79(2)	–	2.82(2)	–
O4w···O12Z	2.822(19)	–	2.820(17)	–

Note: Symmetry Codes: (i) –*x*, –*y*, –1–*z*; (ii) *x*, *y*, –1+*z*; (iii) –*x*, 1–*y*, –*z*; (iv) 1–*x*, 1–*y*, 1–*z*; (v) –*x*, 1–*y*, 1–*z*; (vi) –*x*, 1–*y*, –*z*; (vii) *x*, –1+*y*, –1+*z*; (viii) –*x*, –*y*, –*z*.

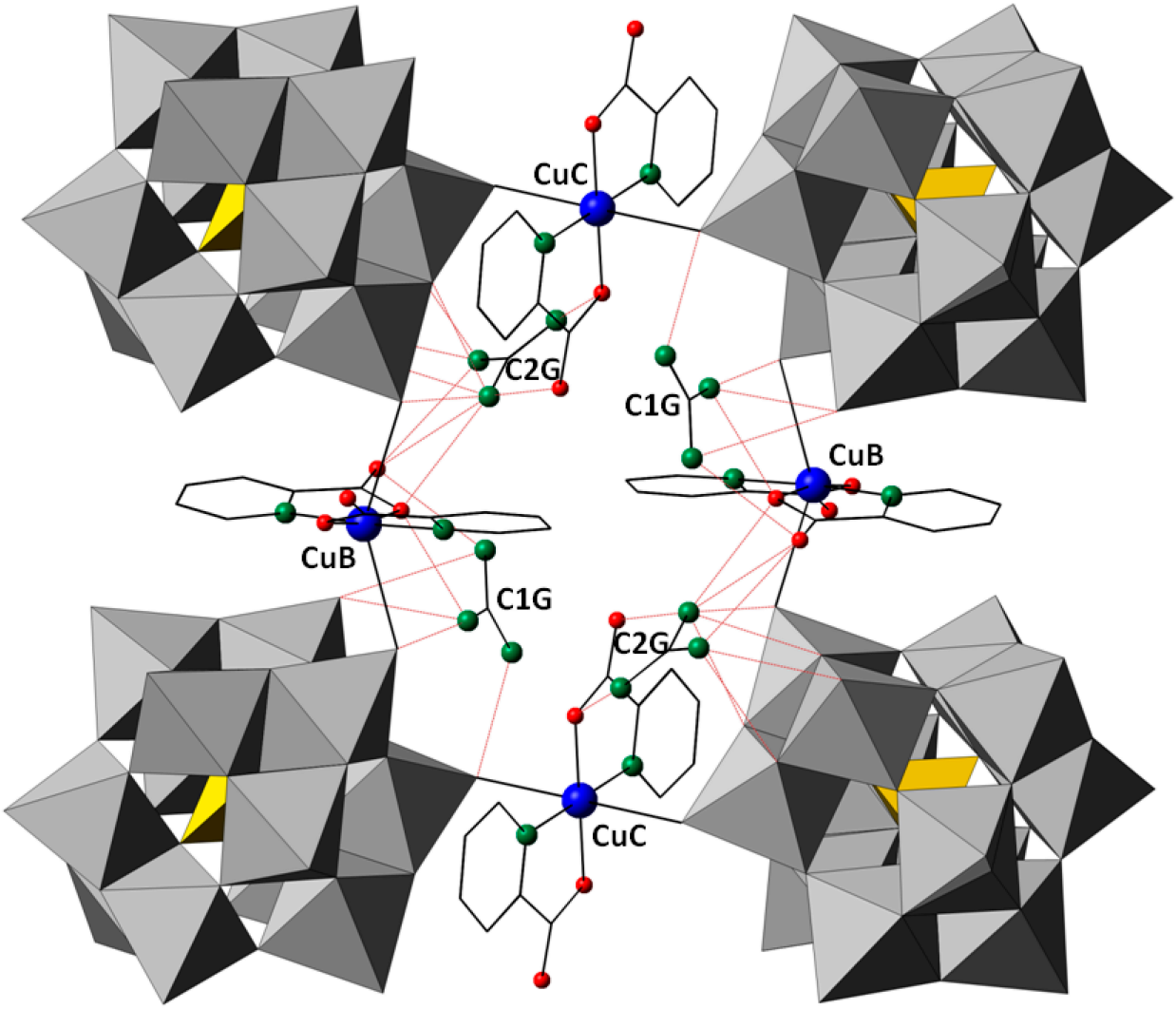

Figure S3. Detail of the N–H···O hydrogen bonds (dotted maroon lines) established by the guanidinium cations C1G and C2G hosted in the rectangular spaces inside the double-chained backbone of the $[\{SiW_{12}O_{40}\}\{Cu(pic)_2\}_{1.5}]_n^{4n-}$ polymer of **2**.

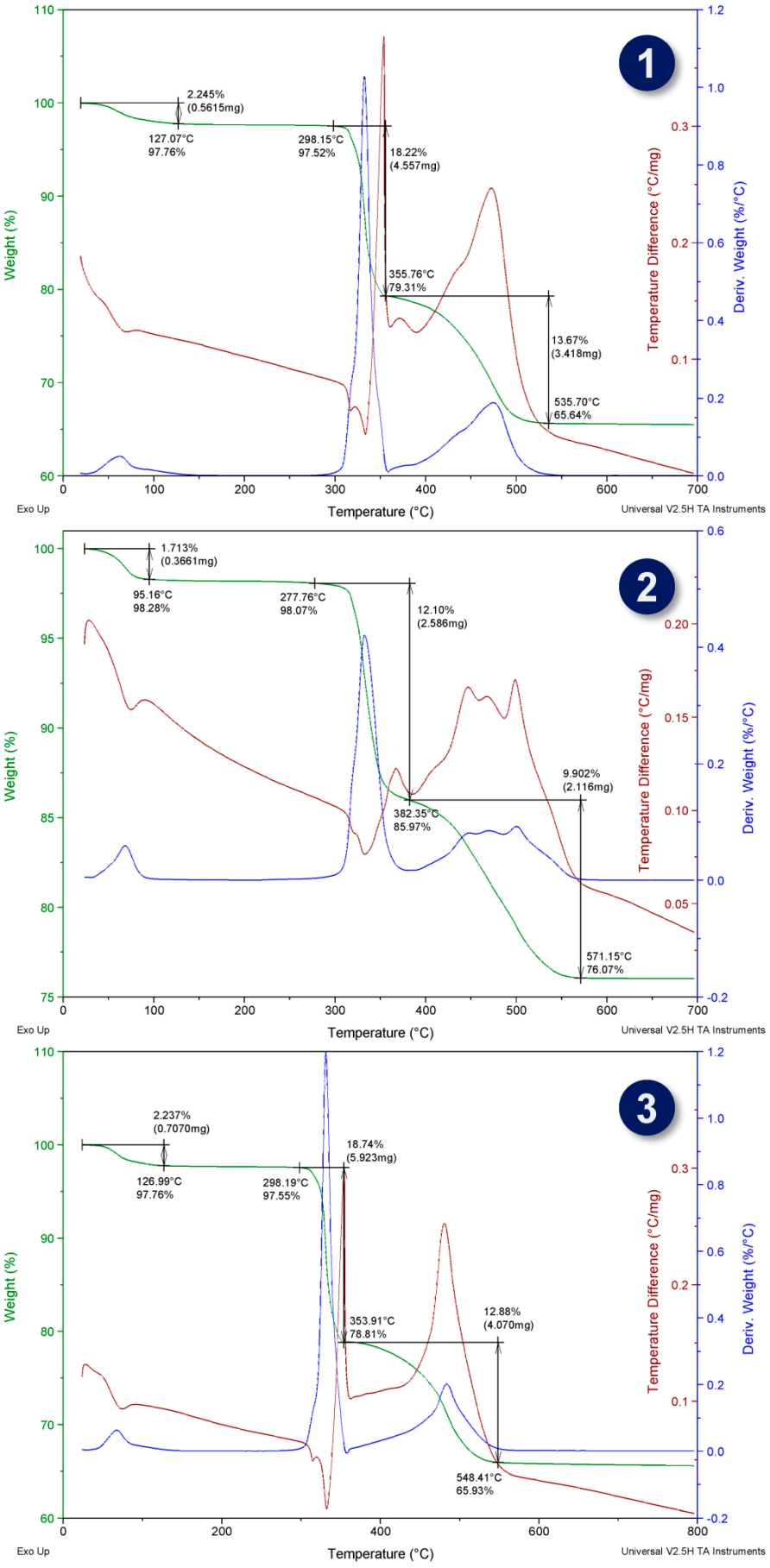

Figure S4. TGA/DTA curves of compounds **1**–**3**.

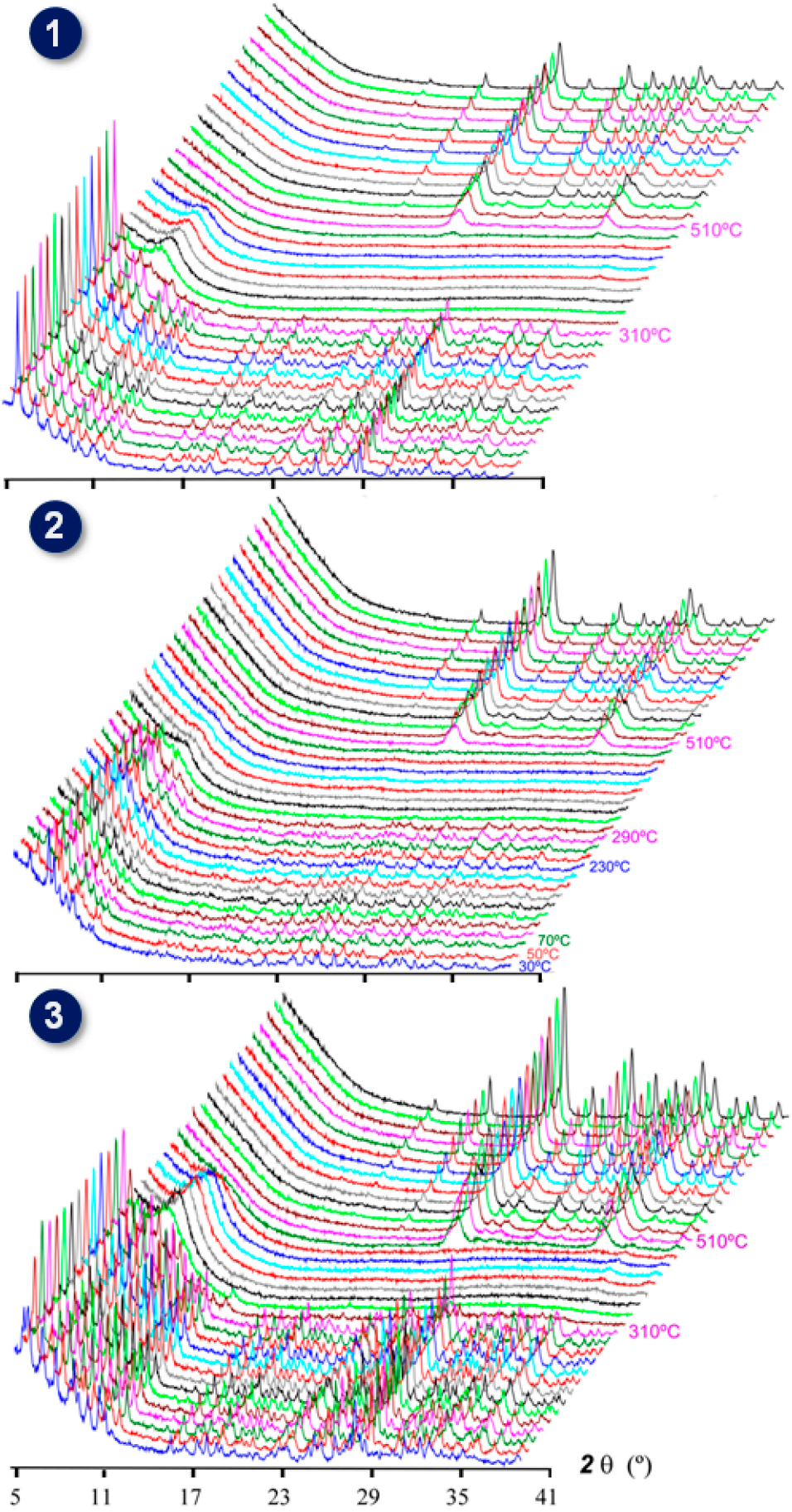

Figure S5. Variable temperature powder X-ray diffraction patterns of compounds **1**–**3**.

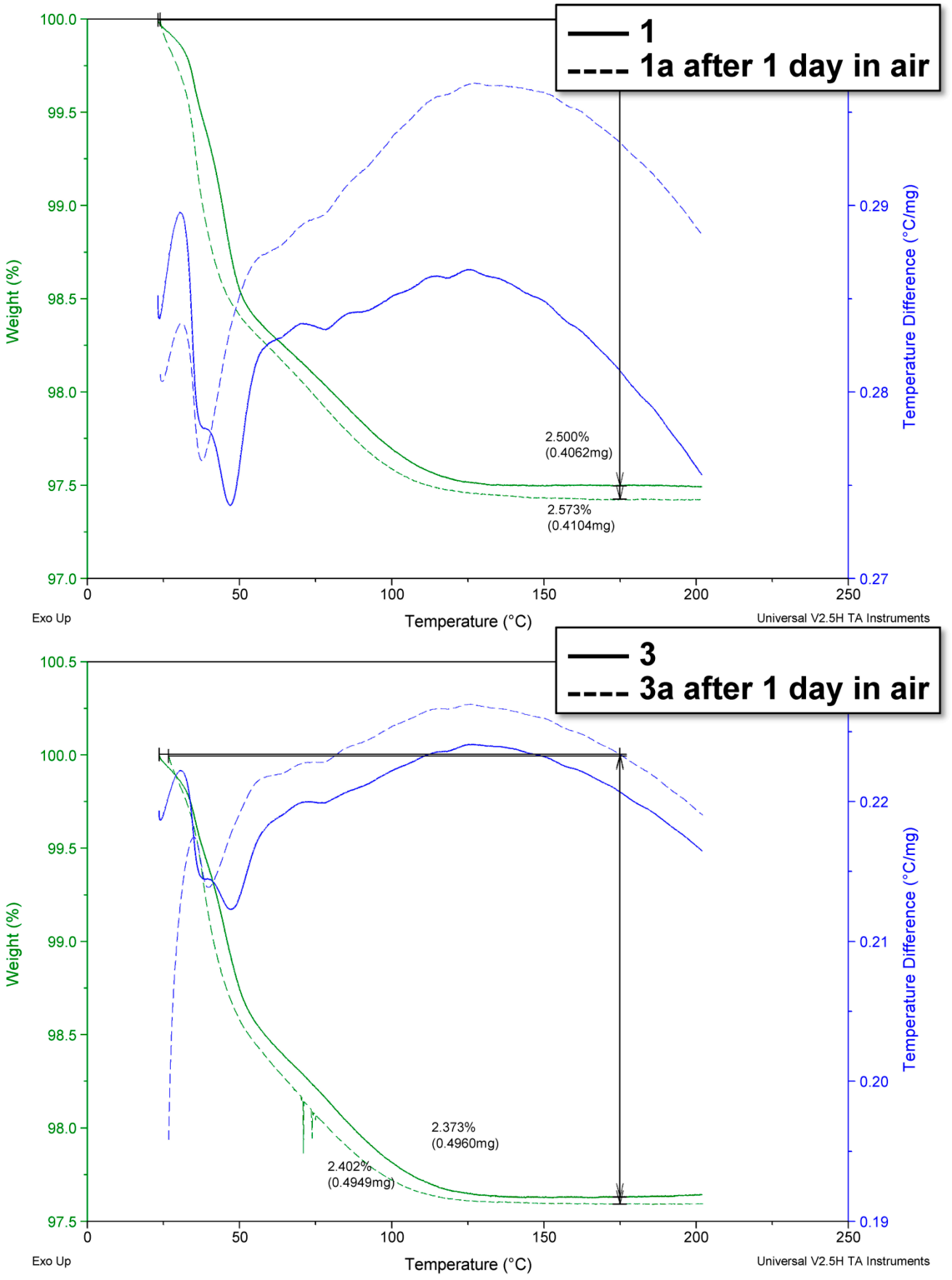

Figure S6. Comparative TGA/DTA curves for the dehydration of compounds **1**/**3** and the resulting phases **1a**/**3a** after being exposed to air for 1 day.

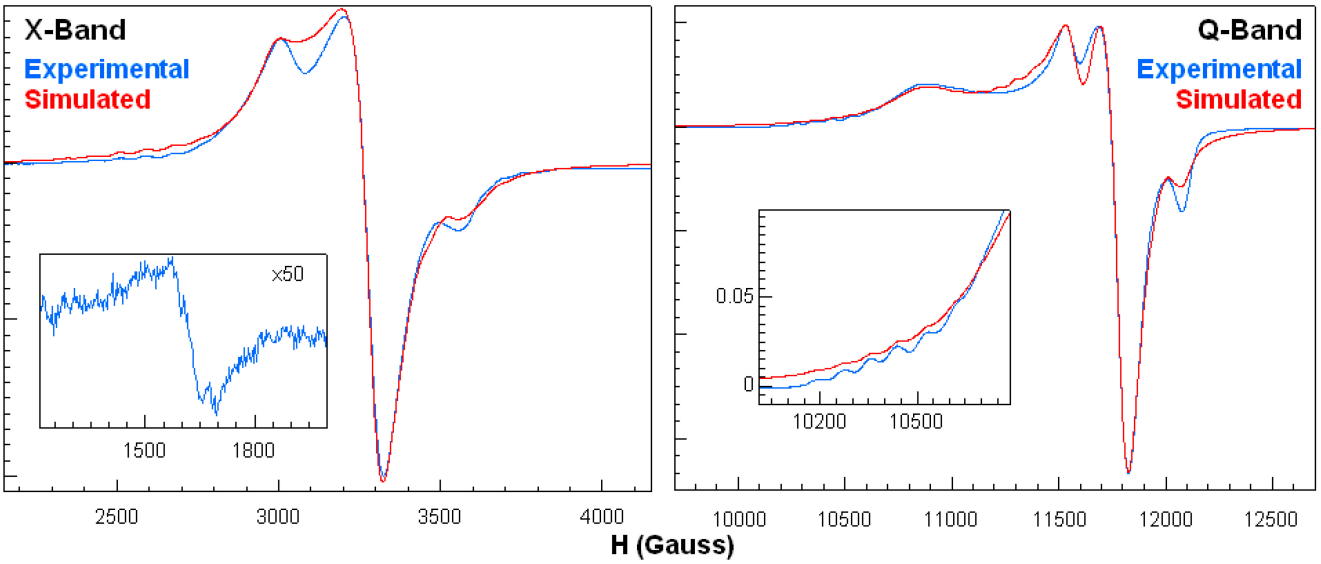

Figure S7. Experimental and simulated X-band (υ = 9.49 GHz) and Q-band (υ = 34.05 GHz) EPR spectra of **3** at room temperature.

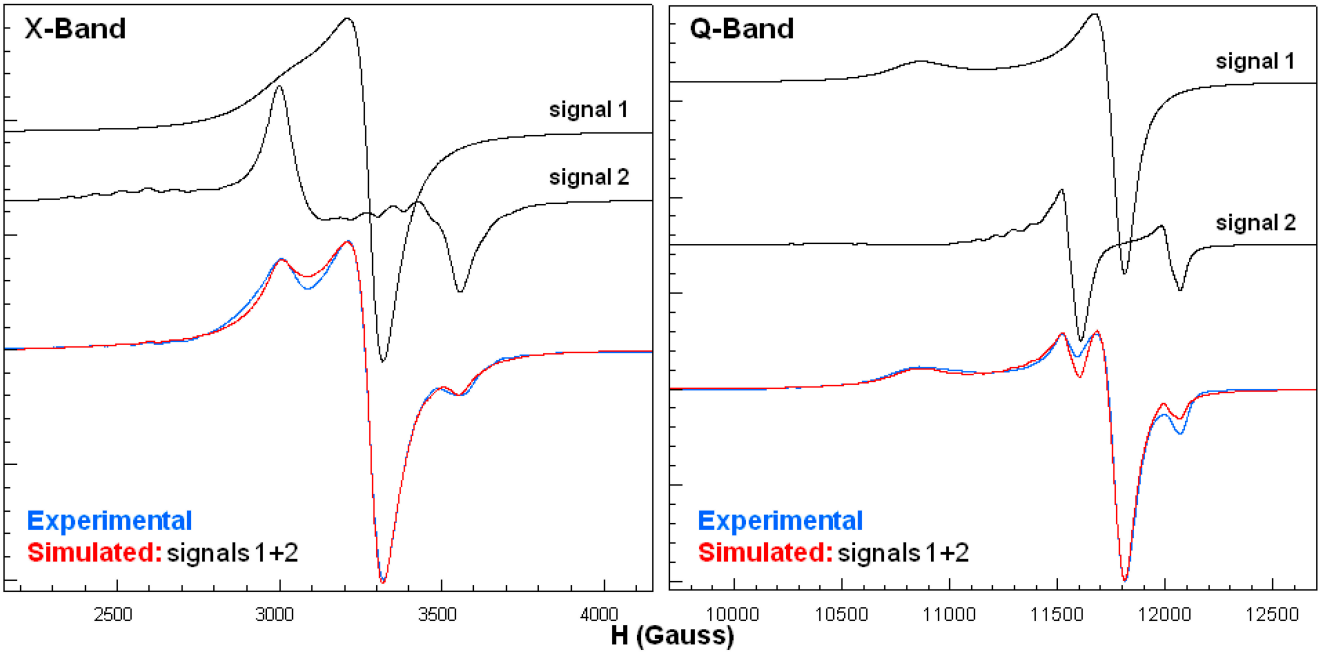

Figure S8. Individual contributions used to simulate the experimental X-band and Q-band EPR spectra of **1** at room temperature.